Mimicking fat grafting of fibrotic scars using 3D-organotypic skin cultures

Raktoe, R.; Kwee, A.K.A.L.; Rietveld, M.; Marsidi, N.; Genders, R.; Quint, K.; ... ; Ghalbzouri, A.E.L.

Received: 23 October 2022 | Revised: 10 July 2023 | Accepted: 17 July 2023

DOI: 10.1111/exd.14893

RESEARCH ARTICLE

Experimental Dermatology WILEY

Mimicking fat grafting of fibrotic scars using 3D-organotypic skin cultures

Rajiv Raktoe[1] | Anastasia K. A. L. Kwee[1] | Marion Rietveld[1] | Nick Marsidi[1] | Roel Genders[1,2] | Koen Quint[1,2] | Remco van Doorn[1] | Paul van Zuijlen[3,4,5,6] | Abdoelwaheb E. L. Ghalbzouri[1]

[1]Department of Dermatology, Leiden University Medical Centre (LUMC), Leiden, The Netherlands

[2]Department of Dermatology, Roosevelt Clinics, Leiden, The Netherlands

[3]Burn Centre, Red Cross Hospital, Beverwijk, The Netherlands

[4]Department of Plastic and Reconstructive Surgery, Red Cross Hospital, Beverwijk, The Netherlands

[5]Department of Plastic, Reconstructive and Hand Surgery, Amsterdam Movement Sciences, Amsterdam UMC (location VUmc), Amsterdam, The Netherlands

[6]Pediatric Surgical Centre, Emma Children's Hospital, Amsterdam UMC, University of Amsterdam, Vrije Universiteit, Amsterdam, The Netherlands

Correspondence
Rajiv Raktoe, Department of Dermatology, Leiden University Medical Centre LUMC, Albinusdreef 2, 2333 ZA Leiden, The Netherlands.
Email: rs.raktoe@gmail.com

Funding information
Nederlandse Brandwonden Stichting

Abstract

Wound healing of deep burn injuries is often accompanied by severe scarring, such as hypertrophic scar (HTS) formation. In severe burn wounds, where the subcutis is also damaged, the scars adhere to structures underneath, resulting in stiffness of the scar and impaired motion. Over the recent years, a promising solution has emerged: autologous fat grafting, also known as *lipofilling*. Previous clinical reports have shown that the anti-fibrotic effect has been attributed to the presence of adipose-derived stromal cells (ADSC). In the proposed study, we aim to investigate the effect of fat grafting in 3D organotypic skin cultures mimicking an HTS-like environment. To this end, organotypic skin cultures were embedded with normal skin fibroblasts (NF) or HTS-derived fibroblasts with or without incorporation of human adipose subcutaneous tissue (ADT) and one part was thermally wounded to examine their effect on epithelialization. The developed skin cultures were analysed on morphology and protein level. Analysis revealed that ADT-containing organotypic skin cultures comprise an improved epidermal homeostasis, and a fully formed basement membrane, similar to native human skin (NHS). Furthermore, the addition of ADT significantly reduced myofibroblast presence, which indicates its anti-fibrotic effect. Finally, re-epithelialization measurements showed that ADT reduced re-epithelialization in skin cultures embedded with NFs, whereas HTS-fibroblast-embedded skin cultures showed complete wound closure. In conclusion, we succeeded in developing a 3D organotypic HTS-skin model incorporated with subcutaneous tissue that allows further investigation on the molecular mechanism of fat grafting.

KEYWORDS
adipose tissue, full-thickness model, (hypertrophic) scars, tissue engineering, three-layered skin model

1 | INTRODUCTION

Deep full-thickness burn wounds are often accompanied by severe scarring, such as hypertrophic scars (HTSs) and can cause substantial functional and aesthetic problems.[1] The underlying mechanism of abnormal scarring is a dysregulation of normal wound healing, as a result of derailed TGF-β signalling.[2,3] During wound healing numerous cell types migrate into the wound bed, including fibroblasts. The fibroblasts differentiate into myofibroblasts in response to TGF-β1 and start expressing alpha-smooth muscle actin (αSMA) and produce collagens, contributing to proper wound closure. Once this process is successfully completed, the myofibroblasts enter apoptosis. However, during severe scarring the myofibroblasts become less responsive towards the apoptotic signals, resulting in the accumulation of fibrotic tissue.[4–6] In addition, in severe burn wounds damage of the skin can reach as far as the subcutis due to the heat penetrating the skin.[7] Surgical removal of the damaged skin reaches up to the muscle fascia and in most cases is restored by split-thickness skin grafts.[8] However, the new scar is still adherent to the tissue underneath. A promising method in the treatment of adherent scars is the use of autologous fat grafting, also known as lipofilling.[7,9–11] Lipofilling is a technique originally used in plastic and cosmetic surgery to correct volume deficiencies due to congenital or traumatic disorders.[12] During this procedure, adipose tissue is grafted underneath the scar tissue. Previous clinical studies have shown that lipofilling successfully reduces the fibrotic characteristics of HTSs and elevating elasticity.[7,13] The anti-fibrotic effect of lipofilling has been primarily attributed to adipose-derived stromal cells (ADSCs) which are described to be pluripotent cells originating from mesenchymal stem cells that reside in subcutaneous adipose tissue throughout the body.[14,15]

Although a few studies have been performed in monocultures and in animal models with ADSCs, the exact molecular mechanism of ADSCs on how they affect HTSs still remains unknown.[16] Therefore, we aim to investigate the effects of fat grafting in a HTS 3D organotypic skin culture. For this purpose, we developed a full-thickness human skin model (FTM) containing adipose tissue (ADT), normal fibroblasts (NF) or HTS-derived fibroblasts, in order to establish a fibrotic environment. In addition, FTMs were cultured with or without the presence of adipose tissue (ADT) and thermally wounded to examine re-epithelialization. First, we assessed the morphogenesis of the three-layered organotypic skin culture compared to our current two-layered skin culture. Next, we determined the effect of ADT on myofibroblast presence and re-epithelialization.

Immunohistochemistry and immunofluorescence analyses showed that epidermal homeostasis and morphogenesis of the three-layered skin culture was improved compared to the two-layered FTMs and featuring more similarities with native human skin (NHS). In addition, fibroblast distribution did not affect basement membrane formation and remained unaffected in ADT-containing skin cultures. Furthermore, ADT-FTMs possessed significantly less myofibroblasts based on αSMA expression. Finally, ADT delayed re-epithelialization in NF-containing FTMs.

In this study, we present a novel 3D three-layered organotypic skin culture that will contribute to a better understanding of the molecular mechanisms of fat grafting. Moreover, this 3D in vitro skin culture may contribute to the development of human skin substitutes in order to treat burn patients.

2 | MATERIALS AND METHODS

2.1 | Cell lines and culture

HTS fibroblasts were isolated from three different HTS biopsies provided by the Red Cross hospital (Beverwijk, Netherlands). Normal human fibroblasts (NF) and keratinocytes were isolated from skin obtained after either mamma reduction or abdominal correction, performed on three female, Caucasian donors. Experiments were conducted in accordance with article 7:467 of the Dutch Law on Medical Treatment Agreement and the Code for proper Use of Human Tissue of the Dutch Federation of Biomedical Scientific Societies (https://www.federa.org/codes-conduct).

NFs and HTS fibroblasts were isolated as described earlier (Table 1).[17,18] In short, the dermis was incubated overnight in dispase II at 4°C and subsequently incubated for 30 min at 37°C for separation of the epidermis from the dermis. Next, the dermal tissues were incubated with collagenase (Invitrogen, Breda, the Netherlands) and dispase (Roche Diagnostics, Almere, the Netherlands), mixed in a 3:1 ratio, for 2 h at 37°C and isolated. The NFs and HTS-derived fibroblasts were cultured in Dulbecco's modified Eagle's medium (DMEM) (Gibco/Invitrogen, Breda, the Netherlands) supplemented with 5% fetal bovine serum (FBS; HyClone, Thermo Scientific, Etten-Leur, the Netherlands) and 1% penicillin–streptomycin (Thermo Fisher Scientific, Massachusetts, United States). The fibroblasts were kept

TABLE 1 Source of human normal fibroblasts, HTS fibroblasts and adipose tissue.

Donor	Sex	Age	Ethnicity	Location
Normal fibroblasts				
1	F	38	Caucasian	Abdomen
2	F	46	Caucasian	Abdomen
3	F	55	Caucasian	Breast
Hypertrophic scar fibroblasts				
1	F	10	Caucasian	Neck
2	M	20	Caucasian	NA
3	M	13	Caucasian	NA
Adipose tissue				
1	F	74	Caucasian	Upper arm
2	F	58	Caucasian	Abdomen
3	F	51	Caucasian	Abdomen

Abbreviations: F: female; HTS: hypertrophic scar; M: male; NA: not available.

at 37°C and 5% CO_2 and used for following experiments between the 3rd and 5th passage.

Keratinocytes were isolated as described earlier.[17] The epidermis from normal skin was incubated with trypsin at 37°C for 15 min. Next, keratinocytes were isolated and cultured in DMEM, Ham's F12 nutrient mixture (Gibco/ Invitrogen, Breda, the Netherlands) supplemented with 5% FBS serum (HyClone/Greiner, Nürtingen, Germany), 5 mL Pen/strep, 0.5 μM hydrocortisone, 1 μM isoproterenol and 5 mg/mL insulin. The keratinocytes were then kept until subconfluency at 37°C and 7.3% CO_2.

ADT was derived from the subcutaneous layer of skin that was obtained from abdominal corrections performed on three female, Caucasian donors (Table 1).

2.2 | Generating full-thickness models

Development of full-thickness models (FTM) consisted of establishment of a dermal and epidermal part. Dermal equivalent preparation was performed using hydrated rattail collagen (4 mg/mL).[19] A 1 mL cell-free collagen mixture with on top a 3 mL collagen mixture embedded with fibroblasts ($1.2–1.5 \times 10^5$ fibroblasts/model) were established onto 6-well filter inserts with a 3 μm pore size membrane (Corning Incorporated, New York, United States). Hydrogels were embedded with either normal skin fibroblasts (NF) or HTS-derived fibroblasts, which will be further referred to as FTM^{NF} and FTM^{HTS}, respectively. Polymerization of both collagen layers was achieved at 37°C. After polymerization, the dermal equivalents were cultured for 1 week in DMEM containing 5% FBS and 1% P/S. Culture medium was changed twice a week. Next, primary keratinocytes were seeded onto the dermal part of the FTM (2.5×10^5 keratinocytes/model). The FTMs were then kept submerged for 4 days followed by culturing at the air–liquid interface for an additional 14 days.[20]

For the generation of adipose tissue (ADT) containing FTMs (ADT-FTM), the ADT was cut into pieces of approximately 5 × 5 mm, after which five pieces were added to the layer of hydrated rattail collagen followed by polymerization at 37°C. The dermal and epidermal part of the ADT-FTMs were established as described above.

2.3 | Morphological and immunohistochemical analysis

For haematoxylin and eosin staining, 5 μm cross sections were stained with haematoxylin for 6 min and eosin for 1 min, to assess the morphology of the different FTMs. Visualization was performed using a light microscope (Zeiss Axioplan 2, Beda, The Netherlands).

Immunohistochemical analyses were performed on 5 μm paraffin-embedded sections. Sections were rehydrated, and antigen retrieval was performed by placing sections in heated sodium citrate buffer. Blocking was done with 2% normal human serum (Sanquin, Leiden, The Netherlands). Sections were incubated with primary antibodies to detect Ki67 (1:100; MIB-1; Agilent, Santa Clara, United States), keratin 10 (1:250; DE-K10; Labvision/ Neomarkers, California, United States), keratin 17 (1:25; CK-E3; Agilent, Santa Clara, United States) and collagen IV (COLIV) (1:150; PHM12; Merck, Darmstadt, Germany) in 1% BSA/PBS at 4°C and secondary antibodies (goat-anti-mouse or goat-anti-rabbit) in 1% BSA/PBS at room temperature. Stainings were visualized with 3-amino-9-ethylcarbazole (AEC) and counterstained with haematoxylin. Sections were enclosed with Kaiser's glycerine and visualized with a light microscope (Zeiss Axioplan 2, Zeiss, The Netherlands).

2.4 | Immunofluorescence staining

Immunofluorescence staining for loricrin (LOR), collagen VII (COLVII), vimentin (VIM) and αSMA was performed on 5 μm thick cryosections. The sections were washed in PBS and fixed in acetone for 10 min followed by blocking in 2% normal human serum for 30 min. Next, sections were incubated O/N at 4°C with primary antibodies targeted against LOR (1:1000; clone# NA; Abcam, Cambridge, United Kingdom), VIM (1:1000; V9; Merck, Darmstadt, Germany) and αSMA (1:500; 1A4/ASM-1; Progen, Heidelberg, Germany). For COLVII (1:150; LH7.2; Abcam, Cambridge, United Kingdom) staining, the sections were incubated with the primary antibody for 1 h at RT. Next, the cryosections were incubated for 1 h at RT with Alexa-488 (1:250; Alexa Flour® Dyes, Thermo Fisher Scientific, Massachusetts, United States) secondary antibody for LOR and Cyanine-3-conjugated secondary antibody (Cy3; 1:600; Jackson ImmunoResearch, Cambridgeshire, United Kingdom) for VIM, αSMA and COLVII. For visualization, the sections were mounted with 4′,6-diamidino-2-phenylindole (DAPI)-containing VECTASHIELD antifade mounting medium (Vector Laboratories Ltd., Peterborough, United Kingdom).

Analysis of αSMA was performed with ImageJ on a fixed area for each sample. The percentage of positive surface was calculated by setting an upper and lower threshold, in order to count the pixels exhibiting a positive fluorescent signal within the boundaries.

2.5 | Masson's trichrome stain

The formalin-fixed paraffin-embedded (FFPE) FTM samples were cut into 5 μm sections, deparaffinized through a series of ethanol baths ranging in concentration from 100% to 50% and continued with the Masson's trichrome stain procedure (Polysciences Inc., Pennsylvania, United States). Next, the sections were re-fixed in Bouin's solution for 1 h at 60°C. Subsequently, the cross sections were stained with Haematoxylin (10 min), followed by Biebrich Scarlet-Acid Fuchsin stain (5 min). The final steps included phosphotungstic/phosphomolybdic acid incubation (10 min) and aniline

blue (5 min). The sections were then dehydrated and mounted with a xylene-based mounting medium. Imaging was performed with a light microscope (Zeiss Axioplan 2, Beda, The Netherlands).

2.6 | Re-epithelialization measurement

The FTMs were thermally wounded as described earlier by Haisma and colleagues.[21] In short, a metal device of 2 mm by 10 mm was cooled in liquid nitrogen for 2 min followed by wounding the FTM for 15 s. No additional pressure was applied during wounding of the organotypic models. After thermal wounding, the FTMs were further cultured for 3 days at the air–liquid interface followed by analysis of re-epithelialization. Haematoxylin and eosin-stained FTM samples were imaged with a light microscope (Zeiss Axioplan 2, Breda, The Netherlands) and relative re-epithelialization was quantified using ImageJ. The relative re-epithelialization was calculated by dividing the length (in pixels) of the newly formed epidermis by the total length (in pixels) of the wound, which was defined by a layer of apoptotic epidermal tissue harbouring small round-shaped cells.[22]

2.7 | Statistical analysis

Data were analysed with GraphPad Prism 7.02 (GraphPad Prism Software, San Diego, CA). Statistical significance was determined by using a Kruskal–Wallis test with a Dunn's multiple comparison post hoc test. The differences were noted as follows: $^{*}p \leq 0.05$; $^{**}p \leq 0.01$; $^{***}p \leq 0.001$.

3 | RESULTS

3.1 | Macroscopic evaluation of developed FTMs and ADT-FTMs

By establishing an ADT-FTM, we first assessed the overall morphology compared to the currently used FTM (Figure 1). A macroscopic view showed that the addition of ADT allowed similar FTM development compared with the two-layered FTMs (Figure 1A). Furthermore, histological images of FTM^{NF}, FTM^{HTS}, ADT-FTM^{NF} and ADT-FTM^{HTS} are depicted in Figure 1B. Comparison of FTM^{NF} versus ADT-FTM^{NF} and FTM^{HTS} versus ADT-FTM^{HTS} showed that the three-layered FTMs presented a dermis onto which a thinner epidermis developed. Here, the presence of the stratum basale, stratum spinosum and stratum corneum are evident. This observation suggests that ADT-FTMs lack a stratum granulosum.

Furthermore, in the ADT-FTMs the subcutaneous layer was properly attached to the dermal compartment. Looking more into detail on the interface between the dermal compartment and ADT, we observed presence of round-shaped cells (black arrows) (Figure 1C). Morphologically similar cells are present in the ADT (red arrows), indicating that these cells have migrated into the dermal compartment. The round cells were not observed in the two-layered FTMs.

3.2 | Effect of adipose-derived tissue on epidermal homeostasis

To evaluate the effect of the modified FTM, we examined epidermal homeostasis of the different FTMs (Figure 2). Therefore, basal cell proliferation (Ki67), early (keratin 10; K10) and late (loricrin; LOR) differentiation and epidermal activation marker keratin 17 (K17) were assessed. Epidermal morphogenesis and organization of the different FTMs were compared to NHS (Figure 2A).

The proliferation of basal cells in ADT-FTM^{NF} was significantly reduced compared to FTM^{NF} ($p \leq 0.01$) based on the differences in the proliferation index (PI). A similar effect on the proliferation was found in FTM^{HTS} where ADT-FTM^{HTS} exhibited a significantly reduced PI compared to FTM^{HTS}. Furthermore, FTM^{NF} and FTM^{HTS} showed a substantial elevation in PI compared to NHS. The three-layered FTMs showed a PI similar to NHS (Figure 2B).

Early differentiation marker K10, showed a clear expression pattern throughout the suprabasal layers in the different FTMs (Figure S1), as found in NHS. As for the late differentiation marker LOR, which is more restricted to the granular layer of the epidermis, we found that ADT-FTM^{NF} showed little to no expression of LOR compared to FTM^{NF}. LOR expression in ADT-FTM^{HTS} samples was downregulated compared to FTM^{HTS}. Furthermore, we observed an overall elevation of LOR expression in FTM^{HTS} compared to NHS. The expression of hyperproliferation marker K17 was slightly elevated in FTM^{HTS} compared to FTM^{NF} and NHS (Figure 2A).

In addition, the effect of ADT on the epidermal thickness was analysed for the different FTMs by calculating the average epidermal area for each sample. In both FTM^{HTS} and FTM^{NF} we found that the addition of ADT significantly reduced the epidermal area (FTM^{NF} vs. ADT-FTM^{NF}, $p \leq 0.05$; FTM^{HTS} vs. ADT-FTM^{HTS}, $p \leq 0.01$) (Figure 2C). Besides reduced epidermal thickness, we also found that ADT-FTMs displayed a thinner and loose stratum corneum compared to the two-layered FTMs (Figure 2D).

In addition, we investigated whether subcutaneous tissue also plays a beneficial role during wound healing (Figure S2). To answer this question, we introduced full-thickness wounds in the different FTMs and assessed re-epithelialization after 3 days. Wounding with liquid nitrogen induced cell death in the injured epidermis in all FTM samples as judged from the small, rounded shape cells, denoted by the black asterisk in the wounded area of the FTMs (Figure S2A–D).[22] In addition, the majority of the fibroblasts in the dermal compartment of FTM^{NF}, ADT-FTM^{NF} and FTM^{HTS} samples did not survive as was observed by small round cells in the wound area, depicted by black arrows (Figure S2A–C).[22] In ADT-FTM^{HTS} cultures most fibroblasts seem to have survived in the full-thickness wound after 3 days (Figure S2D).

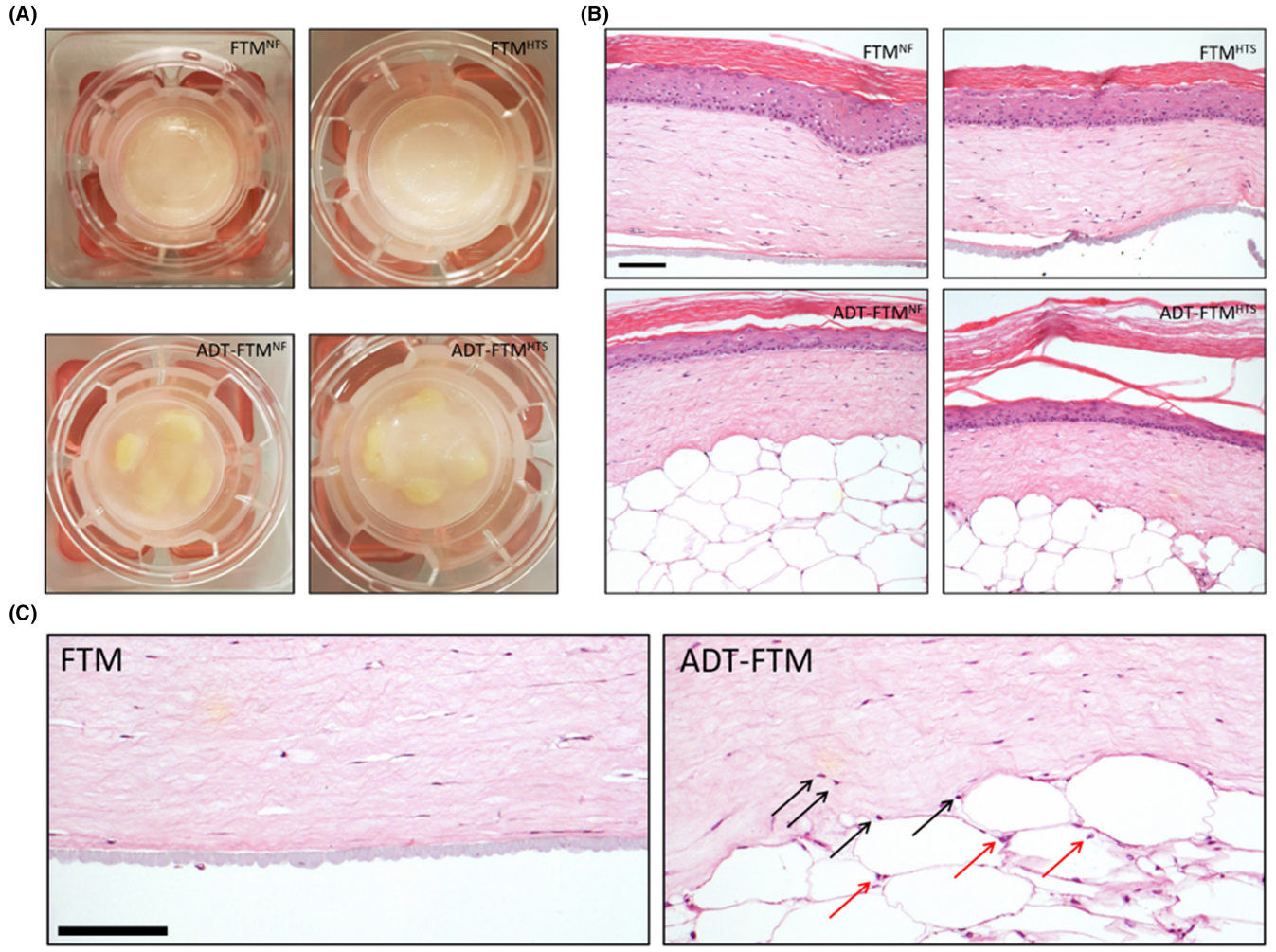

FIGURE 1 Macroscopic images and histology of FTMs. (A) Macroscopic images of FTM^{NF} and FTM^{HTS} formed according to standard protocol (upper images) and with the addition of adipose tissue (ADT): ADT-FTM^{NF} and ADT-FTM^{HTS} (lower images). (B) H and E staining on cross sections of FTMSs established with normal human fibroblasts (FTM^{NF}) ($N=3$), hypertrophic scar-derived fibroblasts (FTM^{HTS}) ($N=3$) displayed in the upper row. The lower row displays the H&E staining of the corresponding FTMs including the addition of adipose tissue: ADT-FTM^{NF} ($N=3$) and ADT-FTM^{HTS} ($N=3$). (C) H and E staining on cross sections displaying the dermal compartment of a two-layered FTM (left). The right image represents the dermal and subcutaneous compartment of the three-layered FTM. In the right image, round-shaped cells are present on the dermal–subcutaneous interface (black arrows). Similar cells are present in the ADT (red arrows). Scale bar: 100 μm.

As shown in Figure S1E, FTM^{NF} showed an average of 94.74% wound closure, whereas ADT-FTM^{NF} samples presented a reduction in re-epithelialization of 24%. Furthermore, all FTM^{HTS}, showed 100% re-epithelialization after 3 days.

3.3 | Fibroblast distribution and effect on basement membrane formation

Next, we determined whether the addition of ADT affects fibroblast presence and basement membrane (BM) formation.[23] Moreover, successful BM formation is essential for proper re-epithelialization and migration of keratinocytes.[22,24–26] Therefore, the expression of BM components COLIV and COLVII was examined by immunohistochemistry and immunofluorescence. As shown in Figure 3, both BM components were present in ADT-FTMs. In addition, immunofluorescence staining for fibroblast marker vimentin (VIM) showed that the fibroblast distribution was similar throughout the different generated FTMs. Furthermore, when comparing fibroblast presence between the different FTMs, we observed that FTM^{NF} samples contained less fibroblasts.

3.4 | The effect of adipose-derived tissue in FTMs on αSMA expression

One of the hallmarks of HTSs is elevated collagen deposition caused by myofibroblast persistence, which are activated by TGF-β1. Since it has been reported that fat grafting reduces collagen deposition through inhibition of TGF-β1 activated fibroblasts, we next investigated whether the addition of ADT could also downregulate activated myofibroblast. Therefore, we determined the expression of myofibroblast marker αSMA by immunofluorescence (Figure 4A).

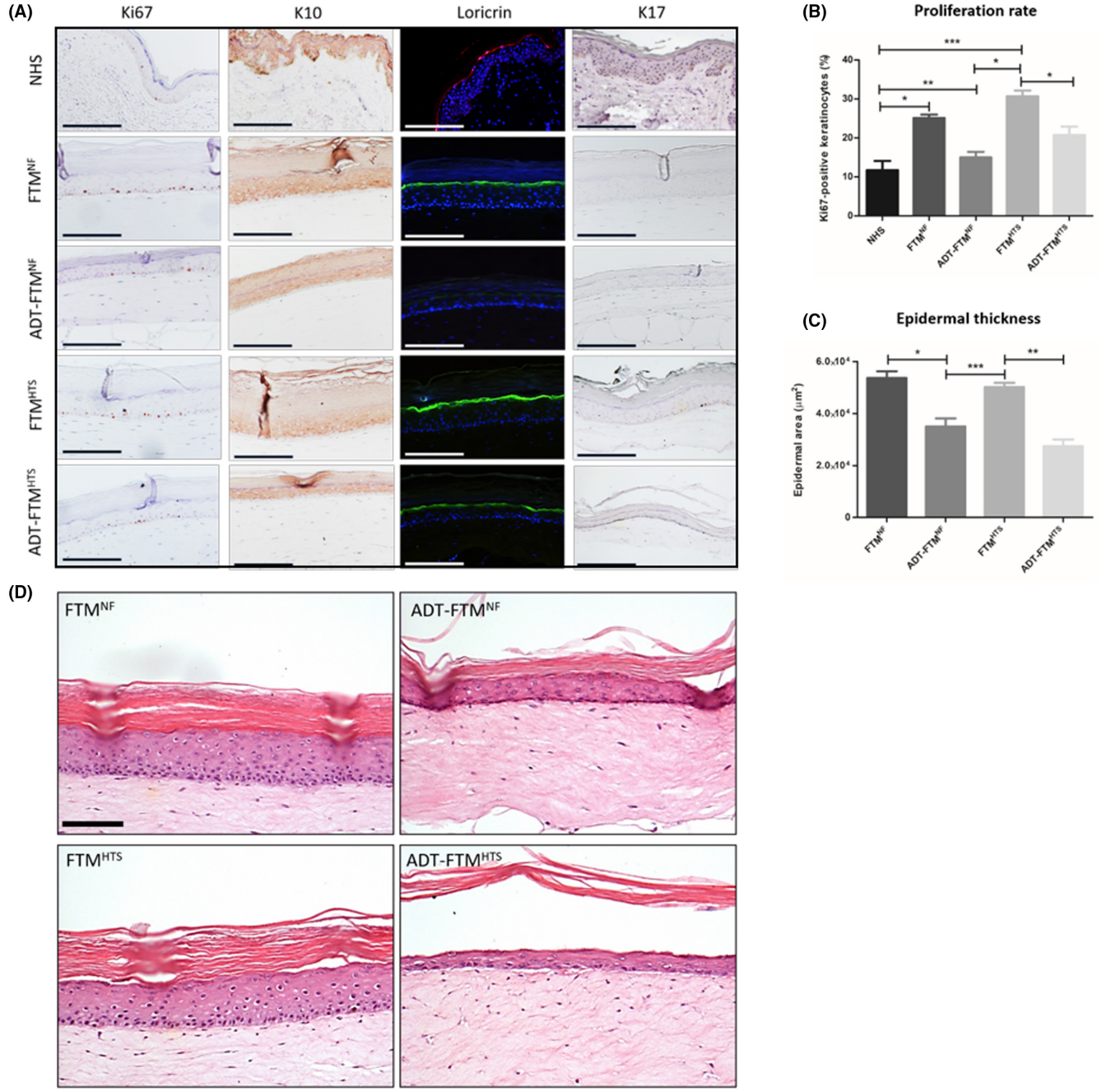

FIGURE 2 Epidermal morphogenesis in NHS, FTM^{NF}, ADT-FTM^{NF}, FTM^{HTS} and ADT-FTM^{HTS}. (A) Immunohistochemistry or immunofluorescence staining for proliferation marker Ki67, early differentiation marker K10, late differentiation marker loricrin and hyperproliferation marker K17. Scale bar: 100 µm. (B) Quantification of the proliferation rate of basal epidermal cells expressed as the percentage Ki67-positive keratinocytes. (C) Quantification of the epidermal thickness expressed as the µm^2 epidermal area. $N = 3$; $^*p < 0.05$; $^{**}p < 0.01$; $^{***}p < 0.001$. (D) H and E staining showing morphological differences in stratum corneum development between FTMs and ADT-FTMs. The three-layered FTMs showed a loose and thinner stratum corneum. Scale bar: 100 µm; $N = 3$.

In FTM^{NF}, the addition of ADT substantially reduced αSMA expression ($p \leq 0.05$). As for FTM^{HTS}, αSMA expression was dramatically downregulated when ADT was added to the FTMs. Although not statistically significant, FTM^{HTS}, showed substantially elevated αSMA expression levels compared to NF-containing skin models (Figure 4A,B).

Another feature of fibrotic dermal tissue is that the collagen bundle orientation shows parallel alignment to one another opposed to a more basket-weave and random bundle orientation in healthy skin.[27] Therefore, we performed a Masson's trichrome stain to visualize the collagen bundles in the different FTMs to assess if incorporation of ADT displays increased waviness (less fibrotic) of the dermal compartment (Figure S3). FTM^{NF} samples presented a similar collagen bundle orientation compared to ADT-FTM^{NF} (Figure S3A,C). Comparison of FTM^{HTS} with ADT-FTM^{HTS} revealed that the addition of ADT resulted in an increase of collagen bundle waviness (Figure S3B,D).

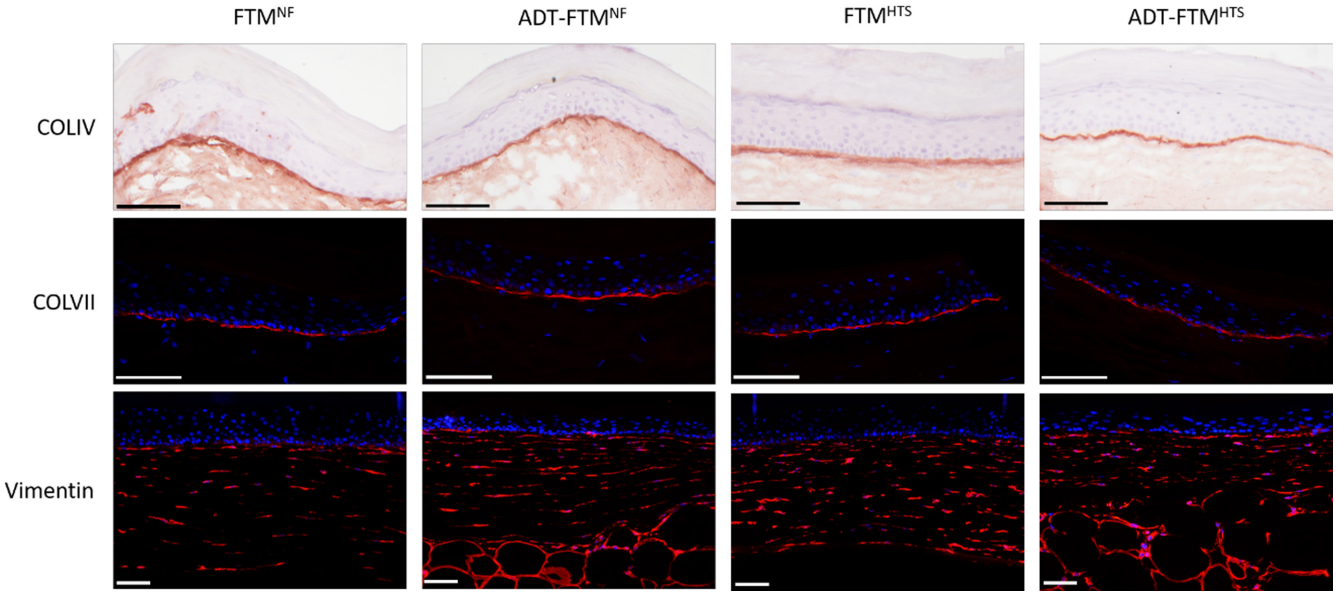

FIGURE 3 Dermal–epidermal junction and fibroblast distribution in the different FTM types. Representative images for COLIV, COLVII and VIM expression in the different types of FTMs: FTM^{NF}, FTM^{HTS}, $ADT\text{-}FTM^{NF}$ and $ADT\text{-}FTM^{HTS}$. The upper and middle row represent deposition of components of the basal membrane COLIV (AEC) and COLVII (fluorescence; red). The lower row displays the expression of vimentin. In the dermal compartment of the FTMs visualized in red by immunofluorescence. For immunofluorescence, the nuclei were visualized using DAPI. Scale bar: 100 μm; $N = 3$.

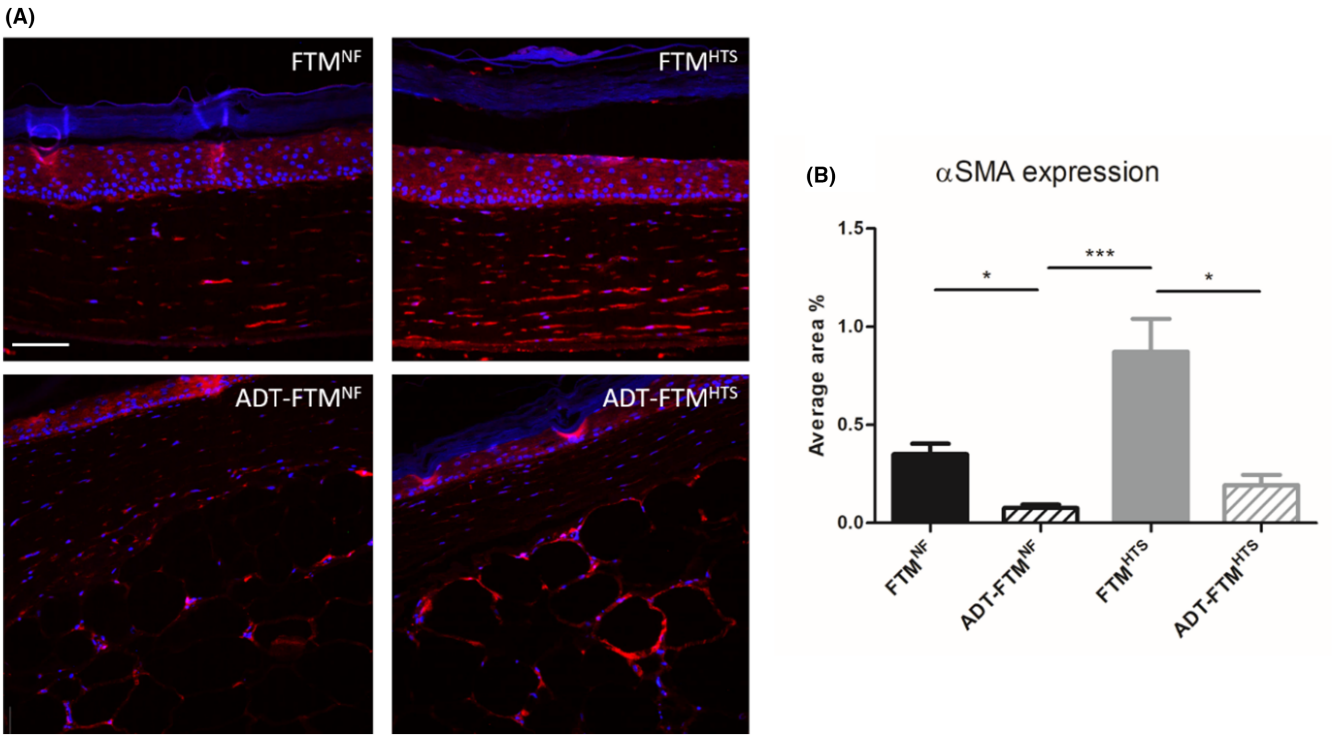

FIGURE 4 Myofibroblast presence in FTM^{NF}, $ADT\text{-}FTM^{NF}$, FTM^{HTS} and $ADT\text{-}FTM^{HTS}$. αSMA immunofluorescence expression in FTM^{NF}, FTM^{HTS}, $ADT\text{-}FTM^{NF}$ and $ADT\text{-}FTM^{HTS}$. (A) αSMA immunofluorescence images of the different FTMS, with αSMA depicted in red and DAPI nuclear staining in blue. Scale bar: 100 μm. (B) Quantification αSMA expression presented as the average positive area percentage. Error bars are presented as standard error of the mean. $N = 3$; $^{*}p < 0.05$; $^{***}p < 0.001$.

4 | DISCUSSION

In this study, we developed a 3D-organotypic model that mimics characteristics of HTSs to elucidate the anti-fibrotic effects of fat grafting. Over the years, several attempts have been made to generate a three-layered skin culture. These studies used isolated adipose stromal cells or mature adipocytes to establish a subcutaneous layer.[28–32] Nevertheless, to our knowledge this is the first study that generated a three-layered human organotypic skin culture using adipose tissue.

Histological examination showed that ADT-containing FTMs display a complete dermal and epidermal developed compartment. However, ADT-FTMs showed a reduction in dermal thickness compared with the two-layered FTMs. We address this reduction to displacement of the dermal compartment due to mechanical pressure exerted by the ADT that is located underneath the dermal compartment of the FTM. The pressure exerted by the ADT did not cause any mechanical stress to the residing fibroblasts in the dermal compartment causing them to differentiate into myofibroblasts as we found that ADT-FTMs showed reduced αSMA expression.[33] As for the epidermis, we observed a reduction in the number of viable layers in ADT-FTMs, resembling epidermal thickness in native skin. Upon investigating epidermal homeostasis, we found that the proliferation rate in ADT-FTMs was significantly reduced compared with non-ADT-containing FTMs and resembled NHS proliferation rate. This result indicates that basal keratinocyte proliferation rate is reduced and, thereby, reduced epidermal thickness.[34,35] Indeed, epidermal thickness was significantly reduced in ADT-FTMs versus the two-layered FTMs. Further investigation on early (K10) and late differentiation (LOR) markers showed that K10 was unaltered in the different FTMs, indicating that the addition of ADT did not interfere with the early differentiation programme. LOR expression, however, was almost absent in ADT-FTM^{NF} samples. This result suggests that the addition of ADT leads to changes in the late differentiation programme and the development of the cornified envelope.[36,37] A possible explanation could lie within in the adipocytokines expression profile, since keratinocytes are also able to respond to these bioactive molecules and thereby affecting epidermal homeostasis including terminal differentiation.[38] However, this hypothesis requires further investigation by starting to assess the secreted adipocytokine profile in the three-layered skin cultures. In addition, further elucidation of epidermal terminal differentiation should include assessment of other terminal differentiation markers, such as involucrin, filaggrin and skin-derived antileukoproteinase (SKALP).[39–41]

Furthermore, when comparing stratum corneum morphology between the different FTMs, we observed in some cases that ADT-containing FTMs exhibited a more loose and thinner stratum corneum. It is warranted to investigate the lipid content and organization of the cornified envelope and stratum corneum, in order to obtain more information on this differential effect.

In a similar study, researchers have established a three-layered FTM by merging the two-layered skin equivalent with a separately cultured hypodermal compartment.[31] In agreement with our study, the three-layered organotypic skin model showed improved epidermal homeostasis, which was comparable with NHS.[31] Additionally, Lu and colleagues constructed an organotypic skin model of which the dermal compartment consisted of a mixture of NFs and ADSCs.[42] The addition of ADSCs improved epidermal morphogenesis of the skin equivalent. These findings raise the option to establish a FTM consisting of a mixture of fibroblasts and adipose stromal cells on the interface between the added adipose layer and the dermis in order to improve communication between the layers. Interestingly, on the interface between the subcutaneous layer and dermal compartment of our ADT-FTMs we observed the presence of round cells (indicated by the black arrows in Figure 1C) that resembled the adipocytes shown in a similar study performed by Huber and colleagues.[32] In this study, the subcutaneous compartment of the three-layered organotypic skin culture consisted of a collagen type I hydrogel embedded with mature adipocytes and detected adipocytes after 7 and 14 days of culturing. Similar cells were detected in the subcutaneous layer of our FTMs and dermal part (indicated by the red arrows in Figure 1C). We hypothesize that mature adipocytes migrated upwards into the dermal compartment and differentiated into fibroblast-like cells, also known as dedifferentiated fat cells.[43,44] Further experimentation is required to confirm this hypothesis, for example by performing multiplexed immunohistochemistry to detect $CD13^+/CD29^+/CD44^+/CD90^+/CD105^+/CD49b^+/CD56^-/CD68^-$ cells to confirm the presence of the dedifferentiated fat cells that resemble dermal fibroblasts and filter out ADT-residing macrophages.[43,45,46]

Another important feature of a viable organotypic skin model is proper development of the BM.[22–26] Therefore, we determined fibroblast presence (VIM) along with major BM collagen components COLIV and COLVII, since deposition of both components is dependent on fibroblast presence.[23] Both BM components were present in ADT-FTMs and in parallel with this finding fibroblast distribution was similar between all FTMs.[23] With regard to fibroblast presence, FTM^{NF} cultures showed less fibroblasts. However, the reduction in fibroblasts did not affect COLIV and COLVII deposition. These results indicate that the addition of ADT did not affect the interplay between the dermal and epidermal layer of the FTMs.

With regard to the potential anti-fibrotic effect of fat grafting, we assessed myofibroblast presence by quantifying αSMA expression. Here we found that in both ADT-FTM^{NF} and ADT-FTM^{HTS} cultures αSMA was significantly downregulated. This anti-fibrotic effect of ADT is primarily addressed to the residing adipose stromal/stem cells, which have been reported to exert their anti-fibrotic effects in a paracrine fashion.[15] Furthermore, previous studies have reported that the anti-fibrotic effect of adipose stromal cell-conditioned medium on NFs and HTS-derived fibroblasts was triggered by reprogramming of myofibroblasts and inhibits TGF-β1-induced fibroblast differentiation resulting in a significant reduction αSMA and collagen type I/III expression.[47,48] In addition to a significant reduction in αSMA-positive fibroblasts, we observed an increase in collagen waviness in ADT-FTMs embedded with HTS fibroblasts, indicating lowered stiffness that in turn could affect MF differentiation through

mechanotransduction pathways (Figure S3).[49–53] These findings are in agreement with previous studies reporting the anti-fibrotic effects of fat grafting of fibrotic scars.[54]

Besides the anti-fibrotic features, fat grafting has also proven to improve outcomes in wound healing studies. Occurrence of cell death in the epidermal and dermal layer as a result of a full-thickness wound was in line with a previous study conducted by our group (Figure S2).[22] However, in ADT-FTM^{HTS} cultures the majority of the fibroblasts seem to have survived in the wound area after 3 days (Figure S2D). One could hypothesize that the combination of the migrating mesenchymal (stem) cells from the ADT could support survival of the HTS fibroblasts. Another explanation could be attributed to displacement of the dermis by the ADT, resulting in a thicker dermis (for some of the samples) underneath the wound area, displaying less damage. Furthermore, we found that the addition of ADT delayed re-epithelialization in FTM^{NF} compared to the two-layered FTMs that contain NFs (Figure S2E). This finding is in line with previous findings from our group in which human skin equivalents were embedded with either NFs or adipose cells.[55] Assessment of epidermal morphogenesis of the latter showed that adipose cells delay the lateral keratinocyte migration rate over a course of 2 weeks. This phenomenon was attributed to elevated presence of myofibroblasts affecting keratinocyte migration.[55,56]

To shift towards a full-functioning human skin equivalent, it is warranted to also include skin appendages such as hair follicles, sebaceous glands and sweat glands.[57] Moreover, studies have shown that stem cells from the skin appendages are involved in epidermal regeneration of the skin after, for example first and second degree burn wounds.[58] The most well-described stem cell niche in the skin is found in the hair follicles. Previous studies have shown that hair follicles contribute to cutaneous wound healing by activation, migration and differentiation of bulge stem cells, fibroblasts and keratinocytes.[58–60] Furthermore, over the past decade studies have shown the regenerative potential of HF-derived dermal papilla cells (DPC) that enable in vitro and in vivo HF growth.[61–63] Here, a proper 3D microenvironment is crucial to maintain the trichogenic capacity of the HF-derived cells.[64] Enabling HF regeneration in our three-layered skin model would be the first step towards a full-functioning skin equivalent that allows investigation of wound healing resembling native skin. A proposed time course to realize HF regeneration in our three-layered skin model, would entail DPC isolation, cell expansion and DP spheroid formation during the first 11 days.[65–67] This is followed by layering the three-layered skin model and incorporation of the DP spheroids into the dermal compartment of the skin model followed by keratinocyte seeding the next day, as described earlier.[61,63] The DP spheroid-bearing three-layered skin model will be cultured on the air-exposed liquid interface for an additional 2 weeks. In theory, one could develop a HF-bearing three-layered skin model in approximately 30 days.

In conclusion, the ADT-FTM showed improved epidermal morphogenesis and did not affect dermal–epidermal communication. Moreover, the addition of ADT induced an anti-fibrotic, as seen upon lipofilling of HTSs. Furthermore, the proposed ADT-FTM in this study could serve as a proper model to further elucidate the molecular mechanisms of fat grafting in hypertrophic scar treatment.

AUTHOR CONTRIBUTIONS

AEG, RR, RG, NM and KQ were involved in the conception and design of the study. PPMVZ performed hypertrophic scar excisions and provided clinical knowledge. AEG and RR designed the experiments. RR and NK carried out the experiments and analysis of the data for this study. The manuscript was written by RR and NK. MHR contributed to the experimental design, immunostainings and data analysis. AEG, RG, NM, KQ and PPMVZ critically reviewed the manuscript.

ACKNOWLEDGEMENTS

None.

FUNDING INFORMATION

This project was funded by the Dutch Burn Foundation (Grant number: NO.14.105).

CONFLICT OF INTEREST STATEMENT

All authors declare that there are no conflicts of interest.

DATA AVAILABILITY STATEMENT

The data that support the findings of this study are available from the corresponding author upon reasonable request.

ORCID

Rajiv Raktoe https://orcid.org/0000-0003-4168-6443

REFERENCES

1. Finnerty CC, Jeschke MG, Branski LK, Barret JP, Dziewulski P, Herndon DN. Hypertrophic scarring: the greatest unmet challenge after burn injury. *Lancet [Internet]*. 2016;388(10052):1427-1436. doi:10.1016/S0140-6736(16)31406-4
2. Schmid P, Itin P, Cherry G, Bi C, Cox DA. Enhanced expression of transforming growth factor-beta type I and type II receptors in wound granulation tissue and hypertrophic scar. *Am J Pathol [Internet]*. 1998;152(2):485-493.
3. Chalmers RL. The evidence for the role of transforming growth factor-beta in the formation of abnormal scarring. *Int Wound J*. 2011;8(3):218-223.
4. Zhu Z, Ding J, Tredget EE. The molecular basis of hypertrophic scars. *Burn Trauma [Internet]*. 2016;4(1):2. doi:10.1186/s41038-015-0026-4
5. Leask AAD. TGF-β signaling and the fibrotic response. *FASEB J [Internet]*. 2004;18(7):816-827.
6. Brown JJ, Bayat A. Genetic susceptibility to raised dermal scarring. *Br J Dermatol*. 2009;161(1):8-18.
7. Jaspers MEH, Brouwer KM, Van Trier AJM, Groot ML, Middelkoop E, Van Zuijlen PPM. Effectiveness of autologous fat grafting in adherent scars: results obtained by a comprehensive scar evaluation protocol. *Plast Reconstr Surg*. 2017;139(1):212-219.
8. Orgill DP. Excision and skin grafting of thermal burns. *N Engl J Med*. 2009;360(9):893-901.
9. Klinger M, Marazzi M, Vigo D, Torre M. Fat injection for cases of severe burn outcomes: a new perspective of scar remodeling and reduction. *Aesthetic Plast Surg*. 2008;32(3):465-469.

10. Negenborn VL, Groen J-W, Smit JM, Niessen FB, Mullender MG. The use of autologous fat grafting for treatment of scar tissue and scar-related conditions: a systematic review. *Plast Reconstr Surg [Internet]*. 2016;137(1):31e-43e.
11. Condé-Green A, Marano AA, Lee ES, et al. Fat grafting and adipose-derived regenerative cells in burn wound healing and scarring: a systematic review of the literature. *Plast Reconstr Surg*. 2016;137(1):302-312.
12. Simonacci F, Bertozzi N, Grieco MP, Grignaffini E, Raposio E. Procedure, applications, and outcomes of autologous fat grafting. *Ann Med Surg*. 2017;20:49-60.
13. Lee G, Hunter-Smith DJ, Rozen WM. Autologous fat grafting in keloids and hypertrophic scars: a review. *Scars Burn Heal*. 2017;3:205951311770015.
14. Mizuno H, Tobita M, Uysal AC. Concise review: adipose-derived stem cells as a novel tool for future regenerative medicine. *Stem Cells*. 2012;30(5):804-810.
15. Borovikova AA, Ziegler ME, Banyard DA, et al. Adipose-derived tissue in the treatment of dermal fibrosis: antifibrotic effects of adipose-derived stem cells. *Ann Plast Surg*. 2018;80(3):297-307.
16. Klinger M, Caviggioli F, Klinger FM, et al. Autologous fat graft in scar treatment. *J Craniofac Surg*. 2013;24(5):1610-1615.
17. El Ghalbzouri A, Commandeur S, Rietveld MH, Mulder AA, Willemze R. Replacement of animal-derived collagen matrix by human fibroblast-derived dermal matrix for human skin equivalent products. *Biomaterials*. 2009;30(1):71-78. doi:10.1016/j.biomaterials.2008.09.002
18. Raktoe RS, Rietveld MH, Out-Luiting JJ, et al. Exon skipping of TGFβRI affects signalling and ECM expression in hypertrophic scar-derived fibroblasts. *Scars Burn Heal*. 2020;6:2059513120908857. doi:10.1177/2059513120908857
19. Smola H, Thiekotter G, Fusenig NE. Mutual induction of growth factor gene expression by epidermal-dermal cell interaction. *J Cell Biol*. 1993;122(2):417-429.
20. Ponec M, Weerheim A, Kempenaar J, et al. The formation of competent barrier lipids in reconstructed human epidermis requires the presence of vitamin C. *J Invest Dermatol*. 1997;109(3):348-355.
21. Haisma EM, Rietveld MH, de Breij A, van Dissel JT, El Ghalbzouri A, Nibbering PH. Inflammatory and antimicrobial responses to methicillin-resistant Staphylococcus aureus in an In vitro wound infection model. *PLoS One*. 2013;8(12):e82800. doi:10.1371/journal.pone.0082800
22. El Ghalbzouri A, Hensbergen P, Gibbs S, Kempenaar J, van der Schors R, Ponec M. Fibroblasts facilitate re-epithelialization in wounded human skin equivalents. *Lab Investig*. 2004;84(1):102-112. doi:10.1038/labinvest.3700014
23. El Ghalbzouri A, Jonkman MF, Dijkman R, Ponec M. Basement membrane reconstruction in human skin equivalents is regulated by fibroblasts and/or exogenously activated keratinocytes. *J Invest Dermatol*. 2005;124(1):79-86.
24. Démarchez M, Hartmann DJ, Herbage D, Ville G, Pruniéras M. Wound healing of human skin transplanted onto the nude mouse. II. An immunohistological and ultrastructural study of the epidermal basement membrane zone reconstruction and connective tissue reorganization. *Dev Biol*. 1987;121(1):119-129.
25. Rigal C, Pieraggi MT, Vincent C, Prost C, Bouisou H, Serre G. Healing of full-thickness cutaneous wounds in the pig. I. Immunohistochemical study of epidermo-dermal junction regeneration. *J Invest Dermatol*. 1991;96(5):777-785.
26. Stanley JR, Alvarez OM, Bere EWJ, Eaglstein WH, Katz SI. Detection of basement membrane zone antigens during epidermal wound healing in pigs. *J Invest Dermatol*. 1981;77(2):240-243.
27. van Zuijlen PPM, Ruurda JJB, van Veen HA, et al. Collagen morphology in human skin and scar tissue: no adaptations in response to mechanical loading at joints. *Burns*. 2003;29(5):423-431.
28. Aoki S, Toda S, Ando T, Sugihara H. Bone marrow stromal cells, preadipocytes, and dermal fibroblasts promote epidermal regeneration in their distinctive fashions. *Mol Biol Cell*. 2004;15(10):4647-4657.
29. Delort L, Lequeux C, Dubois V, et al. Reciprocal interactions between breast tumor and its adipose microenvironment based on a 3D adipose equivalent model. *PloS One*. 2013;8(6):e66284.
30. Monfort A, Soriano-Navarro M, García-Verdugo JM, Izeta A. Production of human tissue-engineered skin trilayer on a plasma-based hypodermis. *J Tissue Eng Regen Med*. 2013;7(6):479-490.
31. Bellas E, Seiberg M, Garlick J, Kaplan DL. In vitro 3D full-thickness skin-equivalent tissue model using silk and collagen biomaterials. *Macromol Biosci*. 2012;12(12):1627-1636.
32. Huber B, Link A, Linke K, Gehrke SA, Winnefeld M, Kluger PJ. Integration of mature adipocytes to build-up a functional three-layered full-skin equivalent. *Tissue Eng Part C Methods*. 2016;22(8):756-764.
33. Tomasek JJ, Gabbiani G, Hinz B, Chaponnier C, Brown RA. Myofibroblasts and mechano-regulation of connective tissue remodelling. *Nat Rev Mol Cell Biol*. 2002;3(5):349-363. doi:10.1038/nrm809
34. Commandeur S, van Drongelen V, de Gruijl FR, El Ghalbzouri A. Epidermal growth factor receptor activation and inhibition in 3D in vitro models of normal skin and human cutaneous squamous cell carcinoma. *Cancer Sci*. 2012;103(12):2120-2126. doi:10.1111/cas.12026
35. van Drongelen V, Danso MO, Out JJ, et al. Explant cultures of atopic dermatitis biopsies maintain their epidermal characteristics in vitro. *Cell Tissue Res*. 2015;361(3):789-797. doi:10.1007/s00441-015-2162-3
36. Nithya S, Radhika T, Jeddy N. Loricrin – an overview. *J Oral Maxillofac Pathol*. 2015;19(1):64-68.
37. Ishitsuka Y, Roop DR. Loricrin: past, present, and future. *Int J Mol Sci*. 2020;21(7):2271.
38. Kovács D, Fazekas F, Oláh A, Törőcsik D. Adipokines in the skin and in dermatological diseases. *Int J Mol Sci*. 2020;21:9048.
39. Watt FM. Involucrin and other markers of keratinocyte terminal differentiation. *J Invest Dermatol*. 1983;81(1 Suppl):100s-103s.
40. Asselineau D, Dale BA, Bernard BA. Filaggrin production by cultured human epidermal keratinocytes and its regulation by retinoic acid. *Differentiation*. 1990;45(3):221-229.
41. Alkemade HA, Molhuizen HO, van Vlijmen-Willems IM, van Haelst UJ, Schalkwijk J. Differential expression of SKALP/Elafin in human epidermal tumors. *Am J Pathol*. 1993;143(6):1679-1687.
42. Lu W, Yu J, Zhang Y, et al. Mixture of fibroblasts and adipose tissue-derived stem cells can improve epidermal morphogenesis of tissue-engineered skin. *Cells Tissues Organs*. 2012;195(3):197-206. doi:10.1159/000324921
43. Matsumoto T, Kano K, Kondo D, et al. Mature adipocyte-derived dedifferentiated fat cells exhibit multilineage potential. *J Cell Physiol*. 2008;215(1):210-222. doi:10.1002/jcp.21304
44. Liao Y, Zeng Z, Lu F, Dong Z, Chang Q, Gao J. In vivo dedifferentiation of adult adipose cells. *PLoS One*. 2015;10(4):e0125254.
45. Dixon AR, Bathany C, Tsuei M, White J, Barald KF, Takayama S. Recent developments in multiplexing techniques for immunohistochemistry. *Expert Rev Mol Diagn*. 2015;15(9):1171-1186.
46. Bornstein SR, Abu-Asab M, Glasow A, et al. Immunohistochemical and ultrastructural localization of leptin and leptin receptor in human white adipose tissue and differentiating human adipose cells in primary culture. *Diabetes*. 2000;49(4):532-538.
47. Spiekman M, Przybyt E, Plantinga JA, Gibbs S, van der Lei B, Harmsen MC. Adipose tissue–derived stromal cells inhibit TGF-β1–induced differentiation of human dermal fibroblasts and keloid scar–derived fibroblasts in a paracrine fashion. *Plast Reconstr Surg*. 2014;134(4):699-712.
48. Hoerst K, van den Broek L, Sachse C, et al. Regenerative potential of adipocytes in hypertrophic scars is mediated by myofibroblast reprogramming. *J Mol Med*. 2019;97(6):761-775.

49. Clark JA, Cheng JCY, Leung KS. Mechanical properties of normal skin and hypertrophic scars. *Burns*. 1996;22(6):443-446.
50. Raktoe RS, van Haasterecht L, Antonovaite N, et al. The effect of TGFβRI inhibition on extracellular matrix structure and stiffness in hypertrophic scar-specific fibroblast-derived matrix models. *Biochem Biophys Res Commun*. 2021;559:245-251.
51. Huang X, Yang N, Fiore VF, et al. Matrix stiffness-induced myofibroblast differentiation is mediated by intrinsic mechanotransduction. *Am J Respir Cell Mol Biol*. 2012;47(3):340-348.
52. Shi-wen X, Thompson K, Khan K, et al. Focal adhesion kinase and reactive oxygen species contribute to the persistent fibrotic phenotype of lesional scleroderma fibroblasts. *Rheumatology*. 2012;51(12):2146-2154. doi:10.1093/rheumatology/kes234
53. Bruno A, Delli Santi G, Fasciani L, Cempanari M, Palombo M, Palombo P. Burn scar lipofilling: immunohistochemical and clinical outcomes. *J Craniofac Surg*. 2013;24(5):1806-1814.
54. Vanderstichele S, Vranckx JJ. Anti-fibrotic effect of adipose-derived stem cells on fibrotic scars. *World J Stem Cells*. 2022;14(2):200-213.
55. El-Ghalbzouri A, Van Den Bogaerdt AJ, Kempenaar J, Ponec M. Human adipose tissue-derived cells delay re-epithelialization in comparison with skin fibroblasts in organotypic skin culture. *Br J Dermatol*. 2004;150(3):444-454.
56. Moulin V, Auger FA, Garrel D, Germain L. Role of wound healing myofibroblasts on re-epithelialization of human skin. *Burns*. 2000;26(1):3-12.
57. Hofmann E, Schwarz A, Fink J, Kamolz L-P, Kotzbeck P. Modelling the complexity of human skin in vitro. *Biomedicines*. 2023;11:793.
58. Xie J, Yao B, Han Y, Huang S, Fu X. Skin appendage-derived stem cells: cell biology and potential for wound repair. *Burn Trauma*. 2016;4:38.
59. Ojeh N, Pastar I, Tomic-Canic M, Stojadinovic O. Stem cells in skin regeneration, wound healing, and their clinical applications. *Int J Mol Sci*. 2015;16(10):25476-25501.
60. Kiani MT, Higgins CA. Almquist BD. The hair follicle: an underutilized source of cells and materials for regenerative medicine. *ACS Biomater Sci Eng*. 2018;4(4):1193-1207.
61. Vahav I, van den Broek LJ, Thon M, et al. Reconstructed human skin shows epidermal invagination towards integrated neopapillae indicating early hair follicle formation in vitro. *J Tissue Eng Regen Med*. 2020;14(6):761-773.
62. Biernaskie J, Paris M, Morozova O, et al. SKPs derive from hair follicle precursors and exhibit properties of adult dermal stem cells. *Cell Stem Cell*. 2009;5(6):610-623.
63. Abaci HE, Coffman A, Doucet Y, et al. Tissue engineering of human hair follicles using a biomimetic developmental approach. *Nat Commun [Internet]*. 2018;9(1):5301. doi:10.1038/s41467-018-07579-y
64. Abreu CM, Marques AP. Recreation of a hair follicle regenerative microenvironment: successes and pitfalls. *Bioeng Transl Med*. 2022;7(1):e10235.
65. Topouzi H, Logan NJ, Williams G, Higgins CA. Methods for the isolation and 3D culture of dermal papilla cells from human hair follicles. *Exp Dermatol*. 2017;26(6):491-496.
66. Higgins CA, Richardson GD, Ferdinando D, Westgate GE, Jahoda CAB. Modelling the hair follicle dermal papilla using spheroid cell cultures. *Exp Dermatol*. 2010;19(6):546-548. doi:10.1111/j.1600-0625.2009.01007.x
67. Higgins CA, Chen JC, Cerise JE, Jahoda CAB, Christiano AM. Microenvironmental reprogramming by three-dimensional culture enables dermal papilla cells to induce de novo human hair-follicle growth. *Proc Natl Acad Sci*. 2013;110(49):19679-19688. doi:10.1073/pnas.1309970110

SUPPORTING INFORMATION

Additional supporting information can be found online in the Supporting Information section at the end of this article.

Figure S1 Enlarged images of suprabasal K10 expression.

Figure S2 The effect of adipose tissue on re-epithelialization in different FTMs.

Figure S3 Application of ADT changes collagen bundle waviness in ADT-FTMHTS.

How to cite this article: Raktoe R, Kwee AKAL, Rietveld M, et al. Mimicking fat grafting of fibrotic scars using 3D-organotypic skin cultures. *Exp Dermatol*. 2023;32:1752-1762. doi:10.1111/exd.14893